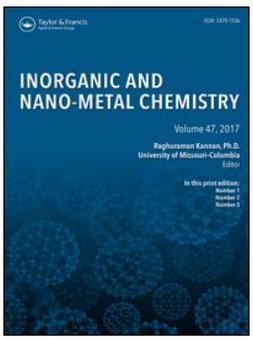

Inorganic and Nano-Metal Chemistry

ISSN: 2470-1556 (Print) 2470-1564 (Online) Journal homepage: https://www.tandfonline.com/loi/lsrt21

Hydrothermal preparation, crystal structure, a series of properties and theoretical calculation of a novel cadmium compound

Yin-Feng Wang, Xiu-Guang Yi, Xiao-Niu Fang, Jia Li, Yao Xu & Shi-Kun Xie

To cite this article: Yin-Feng Wang, Xiu-Guang Yi, Xiao-Niu Fang, Jia Li, Yao Xu & Shi-Kun Xie (2020): Hydrothermal preparation, crystal structure, a series of properties and theoretical calculation of a novel cadmium compound, Inorganic and Nano-Metal Chemistry, DOI: 10.1080/24701556.2020.1735430

To link to this article: https://doi.org/10.1080/24701556.2020.1735430

INORGANIC AND NANO-METAL CHEMISTRY
https://doi.org/10.1080/24701556.2020.1735430

Hydrothermal preparation, crystal structure, a series of properties and theoretical calculation of a novel cadmium compound

Yin-Feng Wang[a], Xiu-Guang Yi[a], Xiao-Niu Fang[a], Jia Li[a], Yao Xu[a], and Shi-Kun Xie[b]

[a]School of Chemistry and Chemical Engineering, Jinggangshan University, Ji'an, Jiangxi, China; [b]School of Mechanical and Electrical Engineering, Jinggangshan University, Ji'an, Jiangxi, China

ABSTRACT

A novel cadmium compound $[CdL(bipy)_2]\cdot 6H_2O$ was synthesized by hydrothermal method, and its crystal structure was determined by single-crystal X-ray diffraction. The title compound crystallized in the monoclinic system of the *C2/c* space group, and existed as an isolated monocyte structure. The strong $\pi \ldots \pi$ stacking interactions produces one-dimensional (1-*D*) chains and a three-dimensional (3-*D*) supramolecular structure is formed by a large number of intermolecular hydrogen bonds . A series of properties of the title compound were tested by solid state photoluminescence, CIE analysis and solid-state diffuse reflectance, and the charge transfer of the title compound was studied by time-dependent density functional theory.

ARTICLE HISTORY
Received 29 December 2019
Accepted 15 February 2020

KEYWORDS
Cadmium; crystal structure; semiconductor; photoluminescence; TDDFT

Introduction

Recently, in the field of chemistry and materials, inorganic-organic hybrid materials have been paid more and more attention by chemists and material scientists, owing to their potential applications in optical materials,[1] semiconductor materials,[2] magnetic materials[3] and medical materials[4] and so on.

Quinoline carboxylic acids are a kind of versatile substance. Many quinoline carboxylic acids possess biological activity, such as antibacterial activities,[5,6] anti-inflammatory and analgesic activity,[7] antileihmanial activity,[8] inhibitors of dihydroorotate dehydrogenase,[9] anticancer activity,[10] and so on. Recently, due to the synergistic effect from coordination modes of quinoline carboxylic acid ligand and anion effect, many quinoline carboxylic acids can be used as the main ligand to construct the supramolecular metal complexes with luminescent activity and biological activity, such as lanthanide complexes,[11] Dy(III) complexes,[12] Cd(II) complexes,[13,14] etc.

Because of the special interest in quinoline carboxylic acids, a series of transition metal complexes with 3-hydroxy-2-methylquinoline-4-carboxylic acid as the main ligand were synthesized and reported by Yi's group, such as, mononuclear Zn(II)/Ni(II)/Pr(III) complexes with monodentate coordination,[15–17] mononuclear Cu(II)/Zn(II) complexes with bidentate chelated coordination.[18–20]

In the continuing of our work, we report here the hydrothermal synthesis, X-ray crystal structure, photoluminescent, and semiconductor properties of the title compound, as well as the calculation of time-dependent density functional theory (TDDFT).

Experimental

Materials and physical measurements

The reagents and chemicals used to synthesize the title compound are analytical reagent grade, which can be sold on the market and can be used without further purification. The infrared spectra is obtained from the PE Spectrum-One Fourier transform infrared (FT-IR), the ^{1}H NMR spectra were measured on Bruker Avance 400 MHz instrument using DMSO as solvent, the photoluminescence was measured on the F97XP photoluminescence spectrometer, the solid-State UV/Vis reflectance spectroscopy was determined with a TU1901 UV/Vis spectrometer equipped with an integrating sphere. TDDFT investigations were performed using the Gaussian 09 suite of program packages.

Synthesis of HL (HL = 3-hydroxy-2-methylquinoline-4-carboxylic acid)

The Synthesis of HL ligands mainly refers to the relevant synthesis literatures, as shown in Scheme 1.[20]

Synthesis of the title compound $[CdL(bipy)_2]\cdot 6H_2O$

The mixture containing HL (203 mg, 1 mmol), $Cd(CH_3COO)_2\cdot 2H_2O$ (170 mg, 1 mmol), bipy (312 mg,

CONTACT Xiu-Guang Yi jayxgggchem@163.com School of Chemistry and Chemical Engineering, Jinggangshan University, Ji'an, Jiangxi 343009, China, Shi-Kun Xie xskun@163.com School of Mechanical and Electrical Engineering, Jinggangshan University, Ji'an, Jiangxi 343009, China.

Supplemental data for this article can be accessed at the publisher's website.

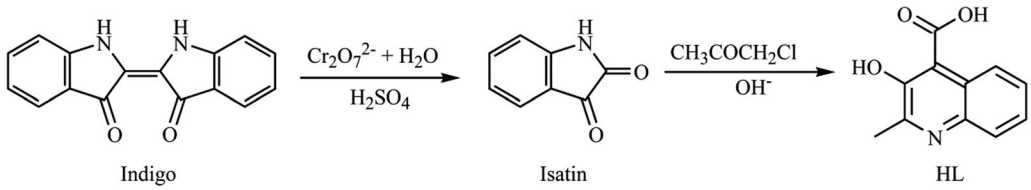

Scheme 1. Synthetic route of ligand HL.

Table 1. Summary of crystal data.

Empirical formula	$C_{31}H_{36}CdN_5O_9$
Formula weight	735.05
Temperature/K	293(2)
Crystal system	monoclinic
Space group	C2/c
a/Å	24.9724(9)
b/Å	17.7565(7)
c/Å	15.3771(5)
α/°	90
β/°	105.862(3)
γ/°	90
Volume/Å^3	6558.9(4)
Z	8
ρ_{calc}g/cm^3	1.489
μ/mm^{-1}	0.726
F(000)	3016.0
Crystal size/mm^3	0.38 × 0.27 × 0.21
Radiation	MoKα (λ = 0.71073)
2Θ range for data collection/°	6.604 to 52.744
Index ranges	$-31 \le h \le 31$, $-22 \le k \le 22$, $-19 \le l \le 19$
Reflections collected	35454
Independent reflections	6698 [R_{int}= 0.0251, R_{sigma}= 0.0190]
Data/restraints/parameters	6698/0/443
Goodness-of-fit on F^2	1.041
Final R indexes [$I \ge 2\sigma$ (I)]	R_1= 0.0367, wR_2= 0.0945
Final R indexes [all data]	R_1= 0.0462, wR_2= 0.1021
Largest diff. peak/hole/e Å^{-3}	1.09/−0.42

$R_1 = \Sigma||F_o|-|F_c||/\Sigma|F_o|$; $wR_2 = \{\Sigma[w(F_o^2-F_c^2]/\ \Sigma[wF_o^2]^2\}1/2$.

2 mmol), H_2O (9 mL), and triethylamine (1 mL) was placed in a 25 mL polytetrafluoroethylene lined autoclave and heated to 100 °C for 7 days under autogenous pressure. When the reaction mixture was cooled down room temperature, bright yellow block-like crystals were obtained, which is used to collect single crystal X-ray data and infrared spectroscopy. The yield was 75% base on $[CdL(bipy)_2]\cdot 6H_2O$. IR peaks (cm^{-1}): 3437(vs), 1631(w), 1595(m), 1562(w), 1434(s), 1355(w), 1310(w), 768(m).

Crystallographic data collection and refinement

The single crystal data of the title compound were collected with a suitable single crystal (size 0.38 mm × 0.27 mm × 0.21 mm) on a SuperNova charge-coupled device (CCD) X-ray diffractometer. During the data acquisition, the crystal temperature was kept at 292(2) K. Using Olex2,[21] the structure was solved with the olex2.solve[22] structure solution program using Charge Flipping and refined with the ShelXL refinement package[23] (using Least Squares minimisation). All of the non hydrogen atoms were generated based on the subsequent Fourier difference diagram and were refined anisotropically. The hydrogen atoms were located theoretically and ride on their parent atoms. The final refining results were given $R = 0.0367$, $wR = 0.0945(w = 1/[\sigma^2(F_o^2) + (0.0506P)^2 + 9.855P])$, where $P = (F_o^2 + 2F_c^2)/3)$; $S = 1.041$, $(\Delta\rho)max = 1.09$ and $(\Delta\rho)_{min} = -0.42$ e/Å^3. Tables 1 and 2 provide a summary of the crystallographic data, selected bond lengths and of the title compound, respectively.

Table 2. Selected bond lengths (Å) and bond angle (°).

Distance	(Å)	Distance	(Å)
Cd(1)–O(1)	2.2330(19)	Cd(1)–N(1)	2.385(2)
Cd(1)–O(2)	2.285(2)	Cd(1)–N(2)	2.356(2)
Cd(1)–N(3)	2.364(2)	Cd(1)–N(4)	2.366(2)
Angle	(°)	Angle	(°)
O(1)–Cd(1)–N(1)	95.71(7)	O(2)–Cd(1)–N(4)	112.04(9)
O(1)–Cd(1)–O(2)	83.64(8)	N(2)–Cd(1)–N(1)	69.56(9)
O(1)–Cd(1)–N(2)	109.98(8)	N(2)–Cd(1)–N(3)	93.48(8)
O(1)–Cd(1)–N(3)	153.99(8)	N(2)–Cd(1)–N(4)	153.51(10)
O(1)–Cd(1)–N(4)	91.65(8)	N(3)–Cd(1)–N(1)	103.08(9)
O(2)–Cd(1)–N(1)	154.28(9)	N(3)–Cd(1)–N(4)	69.56(9)
O(2)–Cd(1)–N(2)	86.21(9)	N(4)–Cd(1)–N(1)	93.68(9)
O(2)–Cd(1)–N(3)	86.93(9)		

Results and discussion

The preparation of the title compound is as follows: first, indigo is oxidized by K_2CrO_7 to form the intermediate product isatin. Second, the ligand HL was obtained by adding chloroacetone to the intermediate isatin in alkaline condition. Finally, the title compound was synthesized by hydrothermal reaction of the HL with cadmium acetate, 2,2′-bipyridine, water and triethylamine. According to the infrared spectrum of the title compound $[CdL(bipy)_2]\cdot 6H_2O$, the strong broad band at 3437 cm^{-1} indicates the presence of water, the absorption at 1631 cm^{-1} is assigned to the contribution of C=N, the absorptions at 1595 cm^{-1} and 1355 cm^{-1} are considered as the presence of monodentated carboxylate in the title compound, as shown in Figure 1.

This compound crystallizes in the monoclinic *C2/c*. The asymmetric unit contains of one cadmium (II) ion, one quinoline carboxylic acid anion, two bipy molecules and six lattice water molecules, as shown in Figure 2. The cadmium atom has hexacoordinated by two oxygen atoms (O(1) and O(2)) from quinoline carboxylic acid and four nitrogen atoms (N(1), N(2), N(3) and N(4)) from two bipys in a distorted octahedron geometry. The Cd (II) ion occupies the center of octahedron, N(1) and O(2) occupy axial position, and N(2), N(3), N(4), O(1) occupy the equatorial plane of octahedron, respectively. The bond distances of Cd–O(1) and Cd–O(2) are 2.2330(19) Å and 2.285(2) Å, respectively, while those of Cd–N(1), Cd(1)–N(2), Cd(1)–N(3) and Cd–N(4) are 2.385(2) Å, 2.356(2) Å, 2.364(2) Å and 2.366(2) Å. These are comparable with that reported in the references.[24,25] Both the quinolinecarboxylate (L–) and bipy

act as the bidentate ligand, which occupy the basal position. The title compound also contains six lattice water molecules. There are not only a A lot of intramolecular hydrogen bonds, which can be found the O–H bond and O atom(O(5)–H(5A)···O(8); O(8)–H(8A)···O(2); O(8)–H(8B)···O(7)), but also a lot of intermolecular hydrogen bonds, which can be found the O–H bond and O atom (O(4)–H(4A)···O(5), (Symmetric code: 3/2 − x, 1/2 + y, 3/2 − z); O(4)–H(4B)···O(9), (1/2 + x, 1/2 + y, z); O(6)–H(6A)···O(5), (3/2 − x,1/2 − y,1 − z); O(7)–H(7A)···O(4), (3/2 − x,1/2 − y,1 − z); O(7)–H(7B)···O(5) (1 − x, −y,1 − z), the N–H bond and O atom (N(5)–H(5)···O(6), (Symmetric code: x, 1 − y, −1/2 + z)) and the O–H bond and N atom(O(6)–H(6B)···N(5), (Symmetric code: x, 1 − y, 1/2 + z)), thus forming a three-dimensional supramolecular structure, as shown in Figure 3 and Table 3, respectively.

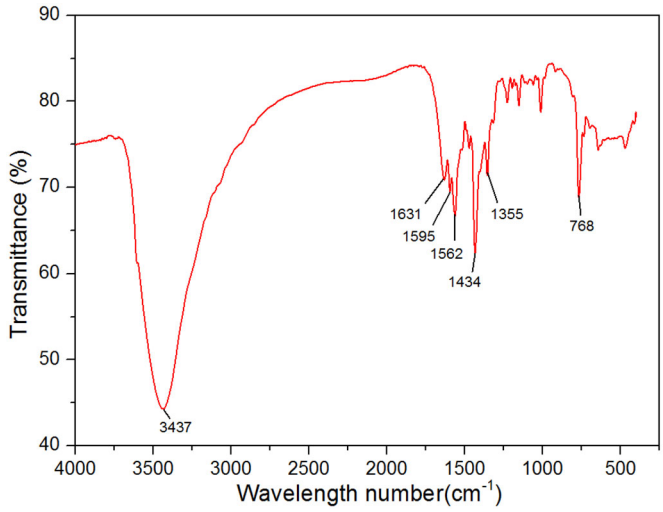

Figure 1. FTIR spectra of the title complex [CdL(bipy)$_2$]·6H$_2$O.

In the title compound, there are also strong offset face-to-face π…π stacking interaction between Cg3···Cg6^{i}, Cg4···Cg5^{ii} [Cg3 is N2/C5/C6/C7/C8/C9, Cg4 is N4/C20/C21/C22/C23/C24, Cg5 is N3/C15/C16/C17/C18/C19, Cg6 is N1/C10/C11/C12/C13/C14; i = 1 − x, 1 − y, 1 − z; ii = 3/2 − x, 1/2x − y, 1 − z]. The centroid–centroid distance of Cg1…Cg6^{i} is 3.629 Å with the shift distance being of 0.275 Å and the twist angle being of 10.528°. The centroid-centroid distance of Cg4···Cg5^{ii} is 3.919 Å with the shift distance being of 1.719 Å and the twist angle being of 177.906°. These π···π stacking interactions and via van de Waals attraction yield the one-dimensional supramolecular structure, the crystal packing as presented in Figure 4. There are also two interactions between C–H···Cg (π···Ring) in the one-dimensional structure, they are C13–H13···Cg8 (N5/C25/C26/C28/C30/C35; x,1 − y,1/2 + z) and C18–H18···Cg8 (N5/C25/C26/C28/C30/C35; 3/2 − x,1/2 − y,1 − z), respectively.

Based on barium sulfate as the reference for 100% reflectivity, the UV–Vis diffuse reflectance spectra of the target compound was measured at room temperature, using the solid-state compound. Data processing adopts $(\alpha h\nu)^{1/n} = A(h\nu - E_g)$, which is the famous Tauc plot formula,[26,27] where α is the absorption coefficient, h is the Planck's constant (6.63×10^{-34}J.s), ν is the frequency, A is the constant and E_g is the band gap of semiconductor. First, the $(\alpha h\nu)^{1/n}$ ($n = 1/2$) and $h\nu$ are obtained by using the solid-state UV–Vis diffuse reflectance spectrum, where $h\nu = hc/\lambda$, λ is the wavelength of light. Second, the graph is draw with $(\alpha h\nu)^{1/n}$ as the vertical coordinate and $h\nu$ (1 eV =

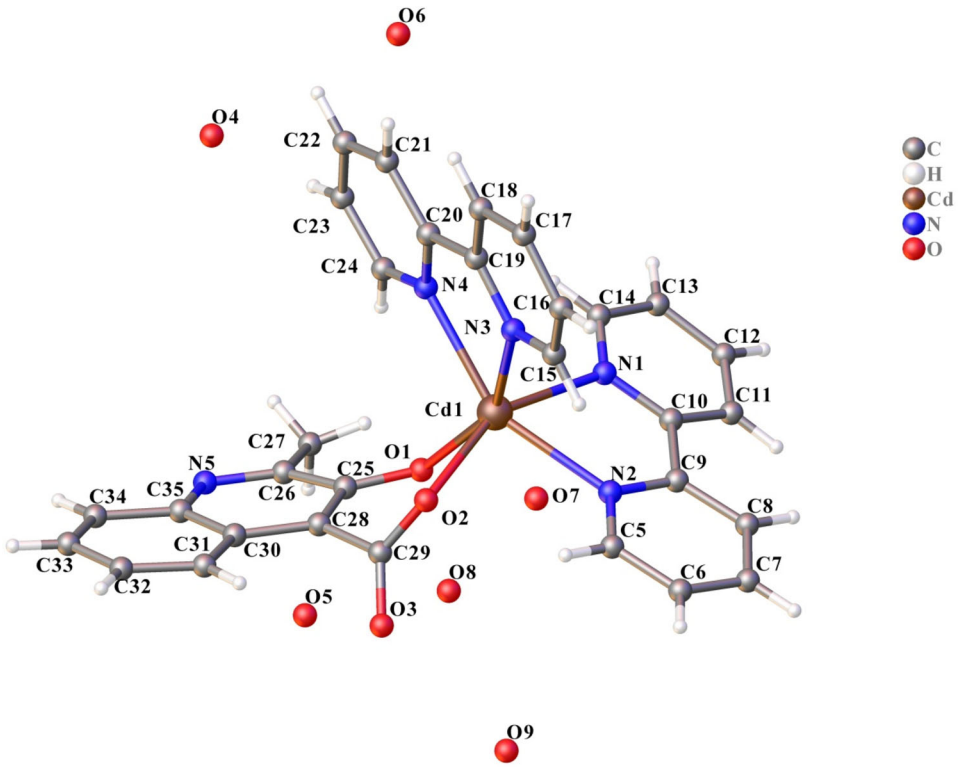

Figure 2. The monomolecular diagram of the title complex. The hydrogen atoms of the lattice water molecules are omitted for clarity.

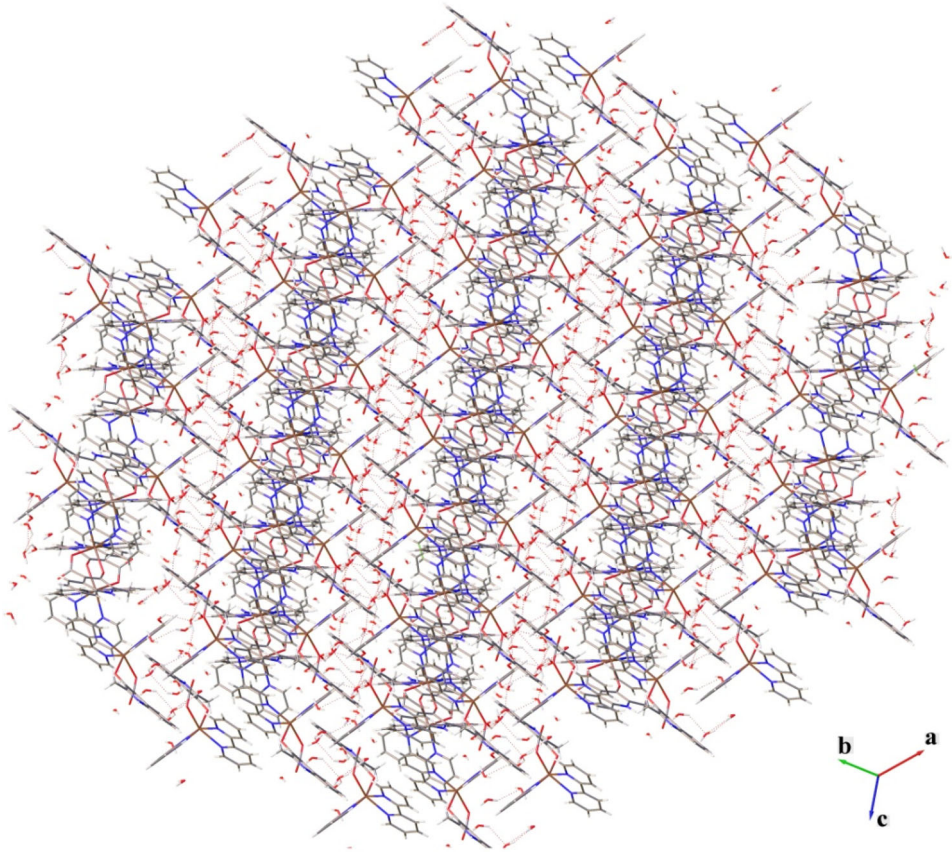

Figure 3. The packing diagram of the title complex with the dashed lines representing the hydrogen interactions.

Table 3. Hydrogen bond lengths (Å) and bond angles (°).

D–H … A	[ARU]	D–H (Å)	H … A(Å)	D … A(Å)	D–H … A (°)
O(4)–H(4A)···O(5)	[6656]	0.85	2.29	2.763(14)	115
O(4)–H(4B)···O(9)	[5555]	0.85	2.36	2.958(16)	128
N(5)–H(5)···O(6)	[4565]	0.86	2.05	2.882(6)	162
O(5)–H(5A)···O(8)		0.85	1.93	2.722(11)	154
O(6)–H(6A)···O(5)	[7656]	0.94	2.05	2.758(10)	132
O(6)–H(6B)···N(5)	[4564]	0.85	2.19	2.882(6)	139
O(7)–H(7A)···O(4)	[7656]	0.85	2.24	2.846(11)	128
O(7)–H(7B)···O(5)	[3656]	0.85	2.14	2.776(11)	131
O(8)–H(8A)···O(2)		0.85	2.32	2.960(8)	133
O(8)–H(8B)···O(7)		0.85	2.27	2.649(14)	107

Symmetric code: [4565] = x, 1 − y, 1/2 + z; [4564] = x, 1 − y, −1/2 + z ; [5555] = 1/2 + x, 1/2 + y, z ; [6656] = 3/2 − x, 1/2 + y, 3/2 − z; [7656] = 3/2 − x, 1/2 − y, 1 − z; [3656] = 1 − x, −y, 1 − z.

1.6×10^{-19} J) as the horizontal coordinate. Finally, the straight part of the figure is extrapolated to the horizontal coordinate, and the intersection point is the energy band gap. As shown in Figure 5, the title compound shows a broad optical energy band gap of 2.61 eV. Therefore, this may be a candidate material for broad band gap semiconductors. The energy band gap of 2.61 eV of the title compound is obviously larger than those of GaAs (1.4 eV), CdTe (1.5 eV), and CuInS2 (1.55 eV),[28–30] those are called efficient band gap photovoltaic materials.

At the same time, in order to reveal the potential photoluminescence characteristics of the title compound, the

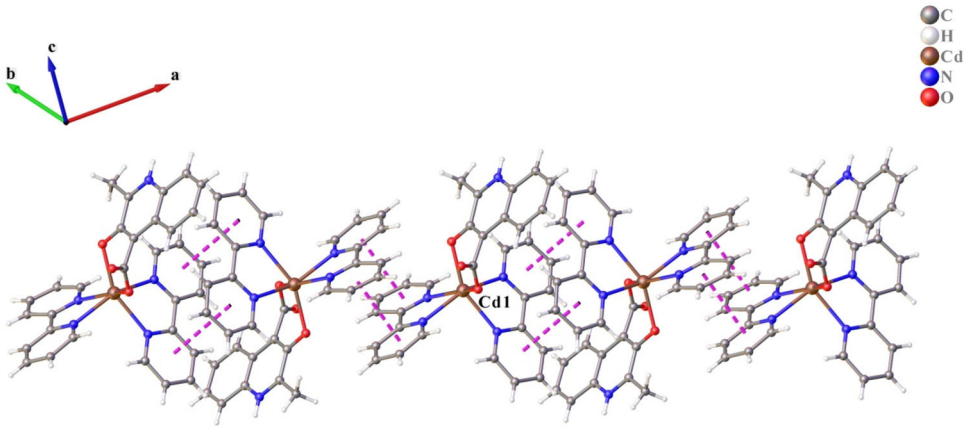

Figure 4. The $\pi \ldots \pi$ stacking interactions diagram of the title complex. The lattice water molecules are omitted for clarity.

photoluminescence spectra of the solid state samples at room temperature were measured, and the results are shown in Figure 6. It can be seen that the photoluminescence spectrum of the title compound shows an effective energy absorption in the wavelength range of 250–470 nm. Upon 445 nm emission, the excitation spectrum shows a band at 522 nm. Under the excitation of 522 nm, there is a sharp band in the blue region of 445 nm. The emission band of the title compound located in the blue region with the CIE1931 chromaticity coordinate (0.1568, 0.0183) (Figure 7). Therefore, the title compound is a potential blue light-emitting material.

In addition, in order to reveal the nature of the photoluminescence properties of the title compound, we truncated ground state geometry from its single crystal X-ray diffraction data set without optimization, and on this basis, we calculated it according to the time-dependent density functional theory (TDDFT). TDDFT calculations were calculated with the nine functions, including B3LYP, B3PW91, mPW3PBE, PBEh1PBE, HSEH1PBE, PBEPBE, M06-L, M06-2X, and BLYP, the base set of SDD for Cd and the base set of 6-31 G* for C, H, O, N, and it were done with the Gaussian09 program.[31] The characteristics of HOMO and LUMO of the title compound are shown in Figure 8. From Table 4, it can be found that the εgap value obtained at TD-B3LYP, TD-B3PW91, and TD-mPW3PBE methods are almost the same. Then, the results at TD-B3LYP method were used in the following discussion. From the figure, we

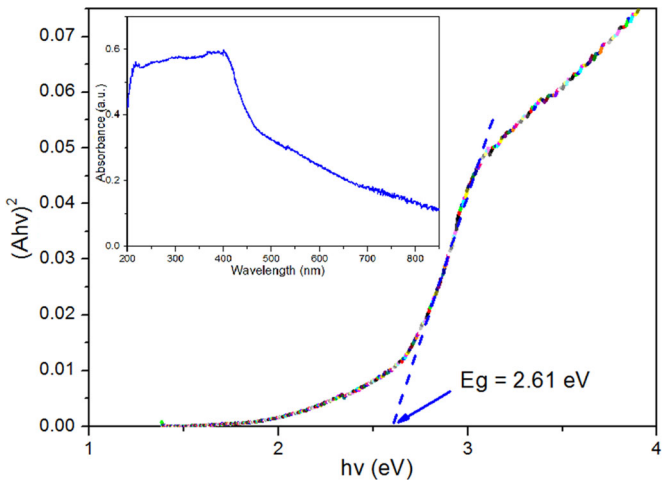

Figure 5. The solid-state UV–Vis diffuse reflectance spectrum (E_g = 2.61 eV). The inset is the UV–Vis spectra of the title complex.

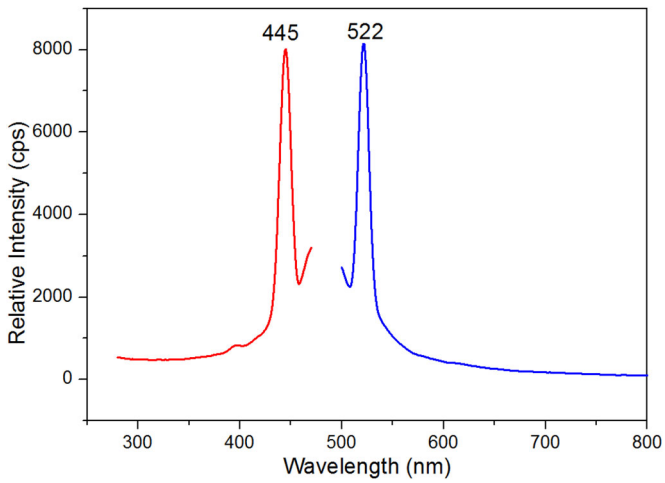

Figure 6. Photoluminescence properties of the title complex (red: emission curve; blue: excitation curve).

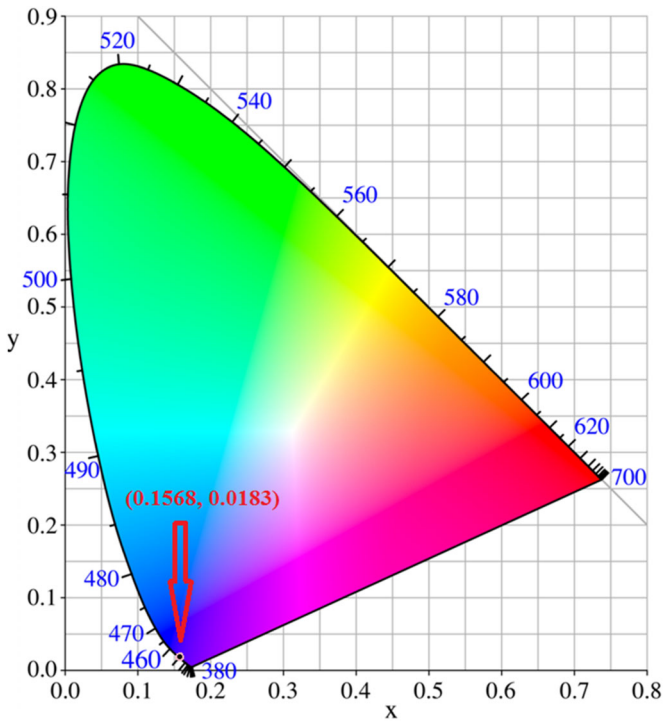

Figure 7. The CIE diagram of the emission spectrum of the title complex.

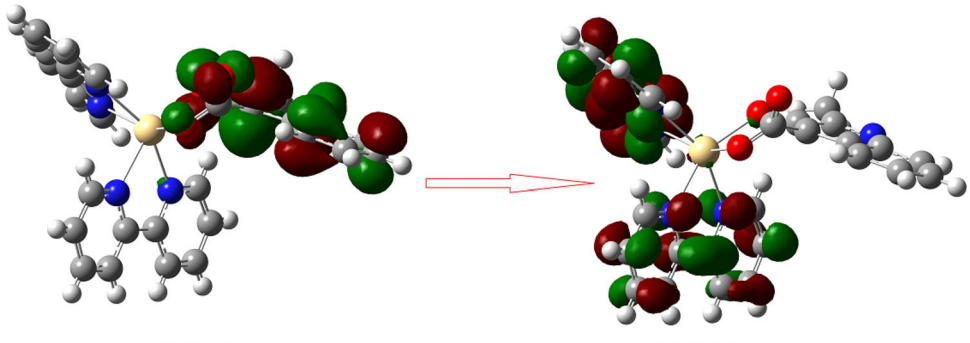

Figure 8. HOMO and LUMO of the title complex with isosurface of 0.03 a.u.

Table 4. Energy of HOMO (ε_{HOMO}, eV), LUMO (ε_{LUMO}, eV), and HOMO-LUMO gap (ε_{gap}, eV) with different methods.

	ε_{HOMO}	ε_{LUMO}	ε_{gap}
TD-B3LYP	−3.448	−2.427	1.020
TD-B3PW91	−3.543	−2.536	1.007
TD-mPW3PBE	−3.554	−2.544	1.010
TD-PBEh1PBE	−3.695	−2.354	1.342
TD-HSEH1PBE	−3.328	−2.713	0.615
TD-PBEPBE	−3.059	−2.898	0.161
TD-M06-L	−3.056	−2.890	0.166
TD-M06-2X	−4.746	−1.595	3.151
TD-BLYP	−2.814	−2.675	0.139

can find that the electron density distribution of HOMO was completely located in the π-orbital of HL with an energy of −3.448 eV (εHOMO); while that of LUMO was completely located in the π-orbital of bipy, with an energy of εLUMO = −2.427 eV. The energy difference (εgap = 1.020 eV) between LUMO and HOMO is small enough to transfer the charge from HOMO to LUMO. According to this observation, we can get that the nature of photoluminescence of the title compound is attributed to the ligand-to-ligand charge transfer (LLCT; from the π-orbital HOMO of ligand HL to the π-orbital LUMO of ligand bipy).

Funding

The work was supported by the National Natural Science of Foundation of China (No.51363009, 1965015), Natural Science Foundation of Jiangxi Province of China(20181BAB206028), Jiangxi Province Department of Education's Item of Science and Technology & Higher Education and Teaching Reform (GJJ190550, GJJ160732, JXJG-17-9-14), Doctoral Research Startup Foundation and Natural Science Foundation Project of Jinggangshan University (JZB1905).

References

1. Chen, H.; Lyu, G.; Yue, Y.; Wang, T.; Li, D.-P.; Shi, H.; Xing, J.; Shao, J.; Zhang, R.; Liu, J. Improving the Photovoltaic Performance by Employing Alkyl Chains Perpendicular to the π-Conjugated Plane of an Organic Dye in Dye-Sensitized Solar Cells. *J. Mater. Chem. C* **2019**, *7*, 7249–7258. DOI: 10.1039/C9TC01520E.
2. Ji, Q.; Li, L.; Deng, S.; Chen, L. High Switchable Dielectric Phase Transition Originating from Distortion in Inorganic–Organic Hybrid Materials (H2dabco-C2H5) [MIICl4] (M = Co, Zn). *Dalton Trans.* **2018**, 47, 5630. DOI: 10.1039/c8dt00623g.
3. Patel, K.; Zhang, J.; Ren, S. Rare-Earth-Free High Energy Product Manganese-Based Magnetic Materials. *Nanoscale* **2018**, *10*, 11701–11718. DOI: 10.1039/C8NR01847B.
4. Wu, T.; Bouř, P.; Andrushchenko, V. Europium (III) as a Circularly Polarized Luminescence Probe of DNA Structure. *Sci. Rep.* **2019**, *9*, 1068. DOI: 10.1038/s41598-018-37680-7.
5. Wang, X.; Xie, X.; Cai, Y.; Yang, X.; Li, J.; Li, Y.; Chen, W.; He, M. Design, Synthesis and Antibacterial Evaluation of Some New 2-Phenyl-Quinoline-4-Carboxylic Acid Derivatives. *Molecules* **2016**, *21*, 340. DOI: 10.3390/molecules21030340.
6. Suresh, N.; Nagesh, H.-N.; Renuka, J.; Rajput, V.; Sharma, R.; Khan, I.-A.; Gowri, C. Synthesis and Evaluation of 1-cyclopropyl-6-fluoro-1,4-dihydro-4-oxo-7-(4-(2-(4-substitutedpiperazin-1-yl)acetyl)piperazin-1-yl)quinoline-3-carboxylic acid Derivatives as Anti-tubercular and Antibacterial Agents. *Eur. J. Med. Chem.* **2014**, *71*, 324–332. DOI: 10.1016/j.ejmech.2013.10.055.
7. Boyarshinov, V.-D.; Mikhalev, A.-I.; Yushkova, T.-A.; Ukhov, S.-V.; Kon'shina, T.-M. Synthesis and Biological Activity of Quinoline-2-Carboxylic Acid Aryl Esters and Amides. *Pharm. Chem. J.* **2017**, *51*, 351–354. DOI: 10.1007/s11094-017-1613-4.
8. Abdelwahid, M.-A.-S.; Elsaman, T.; Mohamed, M.-S.; Latif, S.-A.; Mukhtar, M.-M.; Mohamed, M.-A. Synthesis, Characterization, and Antileishmanial Activity of Certain Quinoline-4-carboxylic Acids. *J. Chem.* **2019**, *2019*, 9. DOI: 10.1155/2019/2859637.
9. Madak, J. T.; Cuthbertson, C. R.; Miyata, Y.; Tamura, S.; Petrunak, E. M.; Stuckey, J. A.; Han, Y.; He, M.; Sun, D.; Showalter, H. D.; Neamati, N. Design, Synthesis, and Biological Evaluation of 4-Quinoline Carboxylic Acids as Inhibitors of Dihydroorotate Dehydrogenase. *J. Med. Chem.* **2018**, *61*, 5162–5186. DOI: 10.1021/acs.jmedchem.7b01862.
10. Bhatt, H. G.; Agrawal, Y. K.; Patel, M. J. Amino- and Fluoro-Substituted Quinoline-4-Carboxylic Acid Derivatives: MWI Synthesis, Cytotoxic Activity, Apoptotic DNA Fragmentation and Molecular Docking Studies. *Med. Chem. Res.* **2015**, *24*, 1662–1671. DOI: 10.1007/s00044-014-1248-x.
11. Zhang, H.-J.; Fan, R.-Q.; Wang, P.; Wang, X.-M.; Gao, S.; Dong, Y.-W.; Wang, Y.-L.; Wang, Y.-L. Structure Variations of a Series of Lanthanide Complexes Constructed from Quinoline Carboxylate Ligands: photoluminescent Properties and PMMA Matrix Doping. *Rsc Adv.* **2015**, *5*, 38254–38263. DOI: 10.1039/C5RA01796C.
12. Bai, J.; Zhang, C.; Tang, J.-X.; Wang, H.-L.; Zou, H.-H. Crystal Structure, Magnetic Properties and Multiplex Photoluminescence of Dy-Exclusive Coordination Polymer Based on Quinoline-2-Carboxylic Acid. *Inorg. Chim. Acta* **2019**, *492*, 182–185. DOI: 10.1016/j.ica.2019.04.027.
13. Zhang, L.; Man, Z.-W.; Zhang, Y.; Hong, J.; Guo, M.-R.; Qin, J. Synthesis, Structure Evaluation, Spectroscopic and Antibacterial Investigation of Metal Complexes with 2-(Pyridin-4-yl)Quinoline-4-Carboxylic Acid. *Acta Chim Slov.* **2016**, *63*, 891–989. DOI: 10.17344/acsi.2016.2895.
14. Pan, G.-H.; Tang, J.-N.; Yin, X.-H.; Xu, W.-J.; Huang, Z.-J. Synthesis, Structures, Electrochemical Analysis, and Luminescence Properties of Four Supramolecular Complexes Based on Quinoline-2-Carboxylic Acid. *Synth. React. Inorg. M.* **2014**, *44*, 848–858. DOI: 10.1080/15533174.2013.791848.
15. Yi, Z.-Q.; Fang, X.-N.; Cao, Z.-Y.; Wei, Y.; Li, Y.-J.; Yi, X.-G. Preparation, Photoluminescence, Semiconductor Properties, and Theoretical Calculations for a Novel Zinc Zero-Dimensional Structure Complex. *J. Chem. Res.* **2019**, *43*, 58–62. DOI: 10.1177/1747519819831886.
16. Fang, X.-N.; Li, J.; Yi, X.-G.; Luo, Q.; Chen, J.-Y.; Li, Y.-X. Preparation, Structure, Photoluminescent and Semiconductive Properties, and Theoretical Calculation of a Mononuclear Nickel Complex with 3-Hydroxy-2-Methylquinoline-4-Carboxylato Ligand. *Acta Chim. Slov.* **2019**, *66*, 414–420. DOI: 10.17344/acsi.2018.4885.
17. Yi, X.-G.; Liu, Y.-Z.; Fang, X.-N.; Zhou, X.-Y.; Li, Y.-X. Crystal Structure and Properties of [PrCl(H_2O)3(L)(HL)]n nCl (HL = 3-Hydroxy-2-methylquinoline-4-carboxylicacid) with One-dimensional Chains. *Chinese J. Struct. Chem.* **2019**, *38*, 325–330. DOI: 10.14102/j.cnki.0254-5861.2011-2065
18. Fang, X.-N.; Li, J.; Yi, X.-G.; Yi, Z.-Q.; Chen, J.-Y.; Li, Y.-X. Synthesis, Crystal Structure, Theoretical Calculation and Properties of Cu(II) Complex with 3-Hydroxy-2-Methylquinoline-4-Carboxylic acid. *Chinese J. Inorg. Chem.* **2019**, *35*(5), 930–936.
19. Li, J.; Shi, L.-S.; Yi, X.-G.; Fang, X.-N.; Guo, T.; Li, Y.-X. Synthesis, Crystal Structure and Catalytic Properties of a 2D Cobalt(II) Coordination Polymer Based on Mixed Ligands. *Chinese J. Struct. Chem.* **2020**,39(3),1–10. DOI:10.14102/j.cnki.0254-5861.2011-2475..
20. Yi, X.-G.; Fang, X.-N.; Guo, J.; Li, J.; Xie, Z.-P. Hydrothermal Preparation, Crystal Structure, Photoluminescence and UV-Visible Diffuse Reflectance Spectroscopic Properties of a Novel

Mononuclear Zinc Complex. *Acta Chim. Slov.* **2020**, *67*. DOI: 10.1734/4.acsi.2019.5532.
21. Dolomanov, O.-V.; Bourhis, L.-J.; Gildea, R.-J.; Howard, J.-A.-K.; Puschmann, H.-J. OLEX2 : A Complete Structure Solution, Refinement and Analysis Program. *J. Appl. Crystallogr.* **2009**, *42*, 339–341. DOI: 10.1107/S0021889808042726.
22. Bourhis, L.-J.; Dolomanov, O.-V.; Gildea, R.-J.; Howard, J.-A.-K.; Puschmann, H.-J. The Anatomy of a Comprehensive Constrained, Restrained Refinement Program for the Modern Computing Environment – Olex2 Dissected. *Acta Crystallogr. A Found. Adv.* **2015**, *71*, 59–75. DOI: 10.1107/S2053273314022207.
23. Sheldrick, G.-M. Crystal Structure Refinement with SHELXL. *Acta Crystallogr. C Struct. Chem.* **2015**, *71*, 3–8. DOI: 10.1107/S2053229614024218.
24. Nallasami, P.; Palanisarmy, R.; Ramaswmy, M. Non-Covalently Aggregated Zinc and Cadmium Complexes Derived from Substituted Aromatic Carboxylic Acids: Synthesis, Spectroscopy, and Structural Studies. *Inorg. Chim. Acta* **2013**, *405*, 522–531. DOI:10.1016/j.ica.2013.04.021.
25. Zhang, X.-J.; Tian, Y.-P.; Li, S.-L.; Jiang, M-h.; Usman, A.; Chantrapromma, S.; Fun, H.-K. Zn(II) and Cd(II) N-Carbazolylacetates with Strong Fluorescence. *Polyhedron* **2003**, *22*, 397–402. DOI: 10.1016/S0277-5387(02)01360-8.
26. Tuac, J.; Grigorovici, R.; Vancu, A. Optical Properties and Electronic Structure of Amorphous Germanium. *Phys. Stat. Sol. (b)* **1966**, *15*, 627. DOI: 10.1002/pssb.19660150224.
27. Davis, E.-A.; Mott, N.-F. Conduction in Non-Crystalline Systems V. Conductivity, Optical Absorption and Photoconductivity in Amorphous Semiconductors. *Philos. Mag.* **1970**, *22*, 903–822. DOI:10.1080/14786437008221061.
28. Lin, W.-S.; Chen, W.-T. Photoluminescence and Semiconductive Properties of a 4f–5d Compound. *J. Iran. Chem. Soc.* **2019**, *16*, 2473–2478. DOI: 10.1007/s13738-019-01715-1.
29. Dűrichen, P.; Bensch, W. K6Nb4S25, the First Ternary Niobium Polysulfide Exhibiting the Complex Anion (Nb4S25)6-: Preparation and Crystal Structure Determination. *Eur. J. Solid State Inorg. Chem.* **1997**, *34*, 1187–1198.
30. Tillinski, R.; Rumpf, C.; Näther, C.; Dürichen, P.; Jeß, I.; Schunk, S. A.; Bensch, W. Synthesis, Crystal Structures, and Optical Properties of New Quaternary Metal Chalcogenides of Group 5: Cs2AgVS4, K2AgVSe4, Rb2AgVSe4, Rb2AgNbS4, and Cs2AgNbSe4. *Z Anorg. Allg. Chem.* **1998**, *624*, 1285–1290. DOI: 10.1002/(SICI)1521-3749(199808)624:8<1285::AID-ZAAC1285>3.0.CO;2-5.
31. Frisch, M.-J.; Trucks, G.-W.; Schlegel, H.-B.; Scuseria, G.-E.; Robb, M.-A.; Cheeseman, J.-R.; Scalmani Barone, G. V.; Mennucci, B.; Petersson, G.-A.; et al. Fox, *Gaussion 09(Revision D.01)*; Gaussian, Inc.: Wallingford, CT, **2013**.